Environmental Earth Sciences (2024) 83:531
https://doi.org/10.1007/s12665-024-11799-5

ORIGINAL ARTICLE

Occurrence, mobility, and potential risk of uranium in an abandoned stone coal mine of Jiangxi Province, China

Xinxiang Wei[1,2] · Naizheng Xu[3] · Li Chen[6] · Jianguang Chen[6] · Jiang Li[4,5]

Received: 2 February 2024 / Accepted: 9 August 2024

Abstract

Metal sulfide oxidation in abandoned exposed stone coal mines leads to the generation of Acid Mine Drainage (AMD), characterized with high uranium concentration, which is a major concern for local public health. This work employed approaches of geochemical analysis and modeling to determined the mode of occurrence of uranium. Additionally, potential environmental risks were evaluated. The results revealed that the primary source of uranium pollutants in the surrounding environmental media was attributed to the weathering of mine wastes. The acidity and concentrations of harmful metals (e.g., U, Fe) and sulfate in water rapidly decreased to background level with increasing distance from the mine. The geochemical distribution characteristics of sediments and water exhibited notable similarities. The species of uranium underwent a transformation as uranium in mine waste rocks migrated to environmental media. In acidic pit water, uranium primarily existed as uranyl sulfate, gradually transitioning downstream to complexes dominated by hydrophosphate and carbonate. This transition was accompanied by the coprecipitation of significant amounts of uranium with phosphate and iron hydroxides. Results from the geoaccumulation index (I_{geo}) and risk assessment codes (RAC) indicated that uranium in unweathered waste rocks and newly formed pit sediments posed a high environmental risk, with a bioavailable fraction reaching up to 26.44% and 48.0%, respectively. This research holds significant importance in devising remediation and management strategies for abandoned coal mines to mitigate the impact of uranium release and mobility on the surrounding ecological environment.

Highlights

- The weathering of stone coal waste is the main source of uranium pollution.
- Newly formed pit poses strong acid generation capacity and high environmental risk.
- The mode of occurrence and environmental conditions determine the mobility of uranium.

Keywords Stone coal · Occurrence and mobility of uranium · Sequential chemical extraction · Environmental risk · Acid mine drainage (AMD)

Introduction

Stone coal, extensively found in the southern regions of China, is a combustible, low-heat value, high-rank sedimentary rock mainly derived from early Paleozoic bacteria and algae after saprofication and coalification in a marine influenced environment. It usually formed before the middle Devonian age (Dai et al. 2017). Covering over 1600 km in a parallel arc in southern China (Steiner et al. 2001), stone coal resources are mainly concentrated in provinces such as Hunan, Zhejiang, Hubei, Anhui, Jiangxi, and Guangxi, with a total reserve of 61,876.7 Mt, almost exclusively distributed in the lower Cambrian (Dai et al. 2017). With large area

✉ Jiang Li
li66001@aliyun.com

1 School of Water Resource and Environmental Engineering, East China University of Technology, Nanchang, China

2 Department of Hydraulic Engineering, Jiangxi Water Resource Institute, Nanchang, China

3 China Geological Survey Nanjing Center, Nanjing, China

4 State Key Laboratory Nuclear Resources and Environment, East China University of Technology, Nanchang, China

5 Teachers' College, East China University of Technology, Nanchang, China

6 Xinjiang Tianshan Uranium Industry Co., LTD, The China National Nuclear Corporation, Urumchi, China

Published online: 02 September 2024

and shallow deposition, most stone coals are open-pit mined near the surface. With the adjustment of national policies, stone coal mines with low caloric value and serious environmental pollution have been gradually closed, resulting in the emergence of a large number of abandoned mines.

Uranium, one of the most common naturally occurring radioactive elements, possesses both chemical toxicity and radioactivity (Chen et al. 2017). It has been established that the presence of organic matter significantly contributes to the enrichment and mineralization of uranium, resulting in the extensive enrichment of uranium within stone coal deposits. According to a study from Qi et al. (2011), stone coal had been identified as an unconventional uranium resource in China. In specific regions, uranium is enriched to the extent of industrial deposits (such as carbon-silica mudstone type) (Wang et al. 2018; Zhang 2000). Moreover, stone coal can be classified as a typical pyrite-type substance and high sulfur coal (Chou 2012), with a total sulfur content ranging from 2 to 4% (mainly pyrite-type sulfur) (Dai et al. 2017). The oxidation and dissolution of pyrite in stone coal due to weathering contribute to the production of AMD, promoting the release of uranium (Lavergren et al. 2009). The weathering of uranium-enriched stone coal is considered a major contributor to uranium pollution in stone coal mining areas (Peng et al. 2004). Therefore, mobility of uranium and the resulting environmental contamination caused by the weathering of uranium-enriched stone coal have attracted significant attention.

A study on the environmental impact of the development and utilization of radioactive stone coal mines in the five provinces of Hubei, Hunan, Anhui, Jiangxi, and Zhejiang, which account for over 90% of stone coal reserves, revealed that the average specific activity of ^{238}U in the soil of mining areas was 370 Bq kg^{-1}, eight times higher than the background average (Ye et al. 2004). In a study conducted by Xu et al. (2018) within the stone coal strata of East China, the monitoring of natural radioactivity levels in air, solid, water, and plant media unveiled that the effective dose of γ-radiation exceeded the threshold (5 mSv a^{-1}). Additionally, the concentrations of total α radiation and total β radiation in groundwater at specific samples exceeded the environmental standard limits by 10 to 30 times (Xu et al. 2018). Radioactive environmental monitoring data obtained by Wei et al. (2021) in a stone coal mining area of Anhui Province, China also indicated that the mean concentration of total α in pit water was 3.27 Bq L^{-1}, exceeding the highest allowable discharge concentration of 1 Bq L^{-1} (Wei et al. 2021). High content of uranium in stone coal mines can seriously threaten ecological and human health, but little is known about how it migrates into the environmental media.

In summary, existing researches have provided valuable insights into the total uranium concentrations in stone coal mines and the surrounding environmental media. However, there remains a lack of information regarding the occurrence of uranium and its potential environmental risk. Indeed, understanding the occurrence of elements is fundamental for deciphering their mobilization processes and evaluating corresponding environmental impacts, with the quantification of trace elements in various chemical fractions holding greater significance than their total concentrations (Zhou et al. 2014).

The sequential chemical extraction method, originally proposed by the European Community Bureau of Reference for heavy metal elements in soils and sediments (Rauret et al. 1989), has been adapted for the quantitative study of the occurrence of trace elements in stone coal (Dong et al. 2018; Lin et al. 2017). This method categorizes element fractions into water-soluble, weak acid-extractable, reducible, oxidizable, and residual fractions. It is widely thought that the sum of water-soluble and weak acid-extractable fractions, known as the bioavailable fraction, is more susceptible to absorb by organisms and transfer through the food chain to humans (Zhang et al. 2021). In contrast, the residual fraction is generally associated with silicate minerals. It is stable in the natural environment and virtually immobile. The toxicity and mobility of harmful elements depend not only on their total concentrations but also on their speciations (Sun et al. 2020). Zhang et al. (2021) and Zhou et al. (2014) attempted to characterize and assess the potential environmental risk of harmful element by using the proportion of the bioavailable fraction (RAC) rather than the total concentration, as the total metal concentration may overestimate the actual level of environmental risk. For instance, weathered soils in Anji, China, showed that although the total Pb content (53.82 mg kg^{-1}) was much higher than that of Cd (1.25 mg kg^{-1}), the stable residual fraction of Pb accounting for 76.34%, while the bioavailable fraction of Cd reached 38.22%. Consequently, Cd posed a higher ecological risk in the area, emphasizing the importance of considering the speciations of harmful elements in environmental risk assessments (Zhang et al. 2021).

Jiangxi, with one of the most abundant stone coal resources in China (predicted total resource reserve of 6834.03 Mt) (Dai et al. 2017), faces challenges associated with open-pit mining, resulting in substantial abandoned waste rocks (average uranium content reported as 100.64 mg kg^{-1}) (Wei and Li 2023a). In the process of weathering, the abandoned waste rocks may release uranium and pollute the local water system and soil. However, there is a lack of understanding of controlling factors for uranium release, migration behaviors, and associated environmental risks. The study's objectives include: (1) determining the mode of occurrence of uranium in stone coal mining area; (2) identifying the source, release and mobility of uranium; and (3)

evaluating the potential risks using I_{geo} and RAC methods. The research results extend our understanding of the source and mobilization mechanism of uranium pollution in abandoned stone coal mine.

Materials and methods

Study area

The research area is situated within Shishi Town and Huanggu Town in Shangrao City, Jiangxi Province, China (Fig. 1). This region typically experiences a subtropical monsoon climate, characterized by elevations ranging from 65 to 331 m. The average temperature is 17.8 °C, and the annual precipitation is 1954.0 mm, indicating of intense chemical and biological weathering. The stone coal-bearing strata is the lower Cambrian Hetang Formation, marked by black thin-layered carbonaceous siliceous rocks, carbonaceous shales, and carbonaceous siliceous shales. The stone coal is deposited in the lower part of the Hetang Formation, consisting of three layers with an average total thickness of 20 m and an average heating value of 5.62 MJ kg^{-1} (Guo 1990). The stone coal forms in a slope environment between the Yangtze Platform and the Jiangnan Deep Sea Basin, developing under anoxic and euxinic conditions (Awan et al. 2020; Wang et al. 2017). Since the 1980s, the stone coal in the research area had been progressively exploited, utilizing on-site combustion for lime production (Guo 1990). This exploitation process has led to significant alterations in the topography, resulting in numerous exposed steep rock walls, open-pits, and piles of stone coal waste rocks (Wei and Li 2023b). These open-pits and abandoned waste rock piles, exposed to the air and acid rain, present potential sources of uranium contaminations. There are two main types of pits with significant differences in formation time, including old pits (more than 20 years old) and new pits (about 3 years old).

Sample collection

In July 2023, a total of 12 stone coal waste rocks were collected in the research area, comprising 2 weathered samples and 10 unweathered samples. Additionally, 26 soil samples

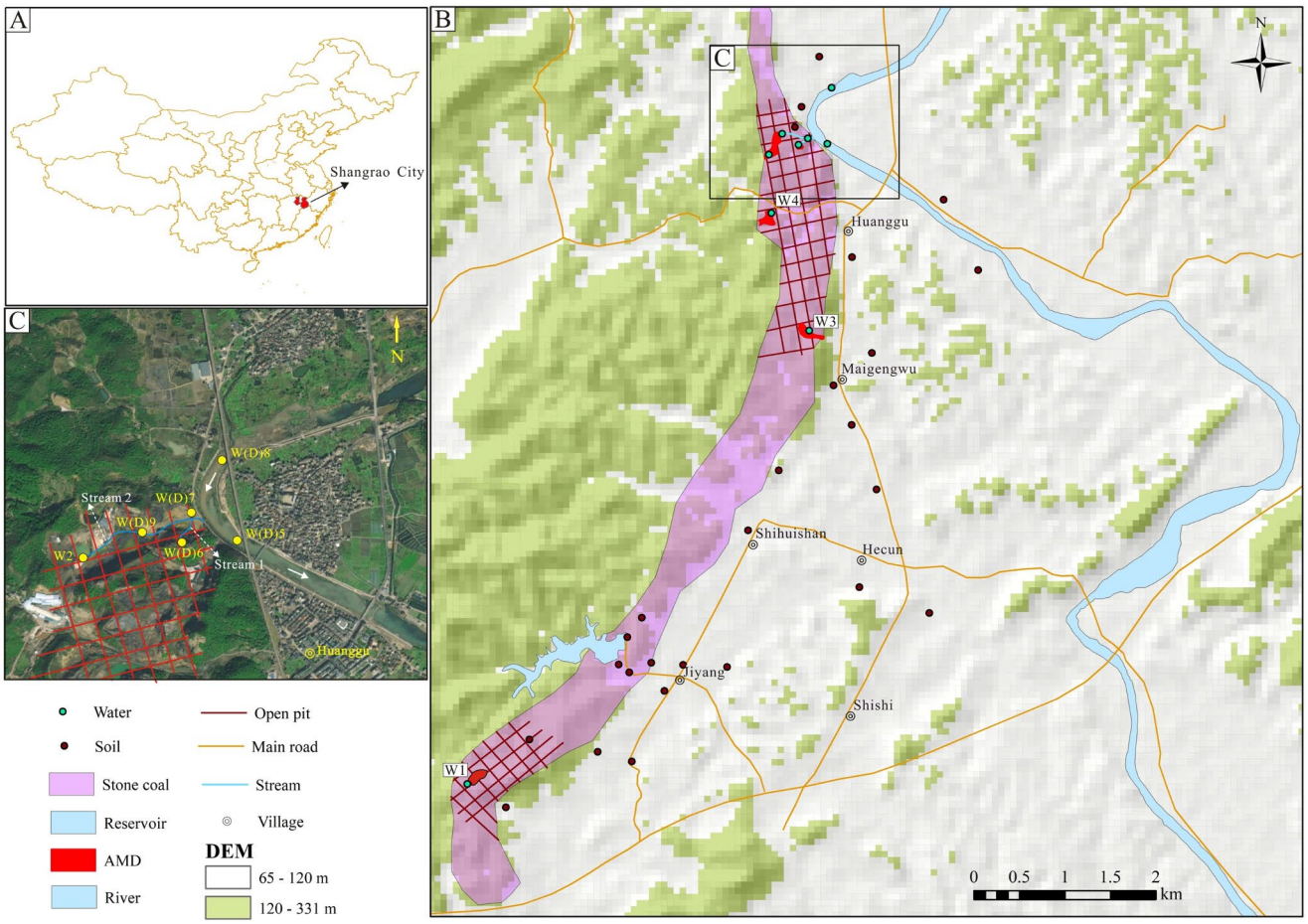

Fig. 1 Geographical location of study area and the distribution of sampling sites

were obtained from farmland, along with 9 surface water samples (including pit water, stream water, and river water) and 5 sediment samples. The waste rocks were sourced from representative open-pit stone coal mining areas, with each sampling point collecting 5 sub-samples randomly to form a composite sample. The sample numbers were prefixed with G (unweathered rocks, G1–G10) and GW (weathered rocks, GW1 and GW7), indicating the degree of weathering as per the method proposed by Peng et al. (2004). In the farmland of the watershed on the eastern side of the stone coal mine, soil samples were collected (prefixed with S, S1–S26). At each sampling point, 5 sub-samples were randomly collected from a 10 m × 10 m plot using a zigzag sampling method, with a sampling depth of approximately 20 cm. Water samples were collected from various sources, including the new pits (W1, W6), old pits (W2–W4), stream flowing through the mining area (W7, W9), and Raobei River (W5). Additionally, river water was collected upstream as a control sample (W8) (Fig. 1). Sediment samples were collected parallel to the stream and river water sampling points, with sample numbers prefixed with DW.

Solid samples, encompassing waste rocks, soils, and sediments, were collected using a quadrant method and sealed in plastic bags for transportation to the laboratory. The samples underwent natural air-drying at room temperature, and after the removal of impurities such as debris and gravel, they were crushed and sieved through a 200-mesh for subsequent analysis. Field measurements of water samples, including pH, Eh, and electrical conductivity (EC), were conducted using a portable multi-parameter water quality meter (YSI ProPlus). All water samples were filtered through a 0.45 μm filter, and stored in two clean polyethylene bottles previously soaked in a 1:1 HNO_3 solution. One bottle was acidified to pH < 2 using HNO_3 for the analysis of major cations and metal elements, and the other bottle was kept as the original sample for the analysis of anions. The collected water samples were stored in a refrigerator at 4 °C and promptly transported to the laboratory for testing.

Chemical analysis

The major elemental oxide content of waste rocks were obtained after lithium borate-lithium nitrate high-temperature fusion, and underwent analysis using X-ray fluorescence spectrometry (XRF, PANalytical PW2424). Total sulfur and total organic carbon (TOC) content in waste rocks and sediment samples were determined using a carbon-sulfur analyzer (LECO CS844). Loss on ignition (LOI) was measured by weighing the samples after calcination at 1000 °C in a muffle furnace. The carbonate and bicarbonate content in sediments were determined by titration according to the standard method LY/T 1251–1999. After digestion with nitric acid, hydrochloric acid, perchloric acid, and hydrofluoric acid, trace elements in solid samples were quantified using inductively coupled plasma optical emission spectrometry (ICP-OES, Agilent 5110) and inductively coupled plasma mass spectrometry (ICP-MS, Agilent 7900). The pH values of soil and sediment samples were determined according to the method specified in NY/T 1377–2007 (Supplementary material), using a pH meter (OHAUS STARTER 3100). For water samples, major cations (Na^+, K^+, Mg^{2+}, Ca^{2+}) and trace elements (Fe and U) were analyzed using inductively coupled plasma mass spectrometry (ICP-MS, LabMS 3000). Major anions (F^-, Cl^-, NO_3^-, SO_4^{2-}) were determined by ion chromatography (IC, Swiss Metrohm 881). Total phosphorus was measured using a ultraviolet-visible spectrophotometer (UV, 1800PC).

Mineral analysis

X-ray powder diffraction (XRD) was utilized to ascertain the mineral composition of both waste rocks and sediment samples. The XRD analysis was conducted using a Japanese Rigaku X-ray diffractometer (Ultima IV) with Cu K-alpha Ni-filtered radiation. The scanning range was set from 5° to 45° (2θ) with a step size of 0.02° and a scanning speed of 2° min^{-1}. Qualitative identification of the main minerals and quantitative analysis of identified minerals were performed using MDI Jade software.

Sequential chemcial extraction method (SCEM)

In addition to determining the total concentration of the radioactive element U, identifying its bioavailable fraction and potential mobility capability is also of significant importance. To understand the occurrence of uranium, a SCEM was employed, following the national standard GB/T 25,282 – 2010, which was revised from the sequential extraction procedure proposed by European Community Bureau of Reference. Through this method, the water-soluble fraction (L_0), weak acid extractable fraction (L_1), reducible fraction (L_2), oxidizable fraction (L_3), and residual fraction (L_4) content of uranium in solid samples such as waste rocks, sediments, and soils were quantitatively determined. The detailed extraction process is outlined in Table S1 of Supplementary material, and the concentration of U in each extract was measured using ICP-MS.

Hydrogeochemical modeling and geochemical mapping

The PHREEQC hydrogeochemical software was utilized to simulate and calculate the species of U in the water samples (using the waterq4f database). ArcGIS 10.2, a geographic

information system, was employed to illustrate the topographical features of the study area, as well as the spatial distribution of sampling points. Additionally, the maps displayed the spatial distribution of U concentration for the soil samples. All maps were created using the WGS 84 geographic coordinate system as the spatial reference.

Results

Mineral and geochemistry of stone coal waste rocks and sediments

Table 1 presents the average mineral compositions of weathered and unweathered waste rocks, revealing significant differences between the two. In unweathered waste rocks (G), quartz dominated the mineral composition (73.0%), followed by calcite, clay minerals, and small amounts of pyrite (3.5%), dolomite, orthoclase, and plagioclase. The mineral composition of the waste rocks changed significantly after weathering, with the content of easily weatherable pyrite decreasing to 0.8% and clay minerals increasing to 12.3%, which may mainly contribute to the weathering decomposition of feldspar (Huang et al. 2017).

Supplementary material Table S2 summarizes the chemical compositions of the waste rocks. The most abundant chemical component was SiO_2, with an average content of 66.09%, followed by CaO, Al_2O_3, MgO, Fe_2O_3, K_2O, and S. The chemical analysis results were consistent with the mineral quantitative analysis conducted using XRD, where Si, Al, Mg primarily associated with quartz and clay minerals, Ca mainly controlled by carbonate minerals (i.e., calcite), K related to feldspar minerals, and Fe and S closely linked to sulfide minerals (such as pyrite). Compared to unweathered waste rocks, the Fe and S content significantly decreased in weathered waste rock, possibly influenced by the oxidation and dissolution of pyrite. The waste rocks demonstrated a high organic matter content, with the content of TOC reaching up to 19.8% and an average of 11.46%. The results of the LOI also supported the conclusion that organic matter was abundant in the waste rock, with an average LOI of 21.09%. Although the organic matter in waste rock is mainly composed of stable organic compounds such as non-degradable n-alkanes and isoprenoids (Zhao et al. 2023), the content of organic matter in weathered waste rock was notably reduced due to long-term weathering. For example, at site G7, the content of TOC decreased from 19.8 to 9.4% after weathering. The uranium concentrations in the waste rocks ranged from 3.6 to 193 mg kg^{-1}, with an average of 84.63 mg kg^{-1}, approximately 35 times the world coal background value (2.4 mg kg^{-1}) (Ketris and Yudovich 2009), indicating a high degree of enrichment. Although there were only 12 samples, the U concentrations in the waste rocks varied, typically with significantly lower concentration in weathered waste rocks (Supplementary material Table S2), indicating the release and mobility of U during weathering processes, as observed by Perkins and Mason (2015).

Hydrochemical characteristics of surface water samples

Table 2 shows the field measurement parameters and chemistry analysis results for water samples. The pH of the new pit water (W1 and W6) was 2.64 and 2.88, respectively, indicating strong acidity. They contained high concentrations of sulfate (3002–5832 mg L^{-1}), metals (Fe, U), and total P, classifying as AMD (Santofimia et al. 2022). Near the new pits, the total sulfur content of waste rocks (G1 and G10) was notably elevated at 2.17% and 4.10% (Supplementary material Table S2), primarily dominated by pyrite. This constituted a key factor triggering the generation of AMD, as pyrite is prone to oxidation under weathering conditions, leading to the formation of AMD (Acharyaa and Kharelb 2020). Due to the longer formation time, the acid generation capacity in the old pits has become limited. After dilution by rainwater and neutralization by surrounding carbonate rocks, the pH approached neutrality (ranging from 6.93 to 7.38), with significantly lower concentrations of sulfate, Fe, U, and total P. As shows in Fig. 1C, acidic pit water (W6) flowed downstream, forming Stream 1 which was reddish-brown and noticeable in the field, but with a lower flow rate. Stream 1 flowed north and converged into Stream 2 which was another stream passing through the mining area, with a flow rate approximately 20 times that of Stream 1. W7 was collected at the confluence point. Stream 2 flowed east and then joined the Raobei River. Due to the strong influence of AMD (W6), downstream W7 also showed significantly high EC (2136 μs cm^{-1}), U (0.404 mg L^{-1}), and low pH

Table 1 The mineral compositions of waste rocks and sediments

Sample	Quartz	Prthoclase	Plagioclase	Calcite	Dolomite	Pyrite	Clay minerals	Ggypsum	Siderite
G	73.0	2.9	0.2	9.3	2.5	3.5	8.6	NMI	NMI
GW	73.8	0.6	NMI[a]	11.2	1.3	0.8	12.3	NMI	NMI
DW6	35.6	1.3	5.0	NMI	0.6	NMI	53.3	3.5	0.7
DW8	42.7	2.9	8.5	NMI	NMI	0.5	44.8	ND	0.6

The unit of all minerals is %. Abbreviations: G and GW refer to unweathered waste rock and weathered waste rock, respectively; NMI, no corresponding mineral identified

Table 2 Hydrochemical characteristics in collected surface water samples

	Guideline value	W1	W2	W3	W4	W5	W6	W7	W8	W9
pH	6–9[a]	***2.64***	7.38	6.93	7.05	7.38	***2.88***	***5.63***	7.77	6.66
Eh	/	550	247	229	270	213	474	251	256	206
EC	/	3830	1538	1306	1464	291	5590	2136	291	1878
Na^+	/	0.292	53.9	2.57	3.74	2.32	0.626	47.2	1.79	50.3
Mg^{2+}	/	1.11	19.4	22.5	28.6	2.23	144	25.8	2.00	22.2
K^+	/	0.733	7.43	4.05	3.27	1.26	0.425	68.6	1.10	7.21
Ca^{2+}	/	21.5	19.8	17.2	23.3	1.90	47.8	28.9	1.55	28.6
SO_4^{2-}	250[a]	***3002***	***853***	***689***	***980***	9.30	***5832***	***1276***	11.1	***1077***
HCO_3^-	/	bdl	50	35	47	51	bdl	47	55	48
Cl^-	250[a]	85.18	46.61	60.53	27.81	50.07	20.84	123.3	51.40	72.11
NO_3^-	10[a]	0.913	2.28	0.535	0.937	3.56	bdl	1.40	4.11	2.28
F^-	1[a]	***2.10***	***7.18***	0.314	0.973	0.248	***16.5***	***5.98***	0.250	***5.36***
Fe	0.3[a]	***193***	***0.385***	0.228	0.288	0.188	***400***	***18.5***	0.116	***0.505***
total P	0.2[a]	***2.26***	0.010	0.007	0.013	0.029	***6.54***	***0.422***	0.030	0.002
U	0.03[b]	***0.390***	***0.039***	0.019	***0.046***	0.128×10^{-2}	***8.69***	***0.404***	0.125×10^{-2}	***0.050***

The units of pH, Eh, and EC are dimensionless, mV, and μs cm^{-1}, respectively. Other parameters are mg L^{-1}. [a] Guideline values are referenced from the Surface Water Environmental Quality Standards (GB 3838 – 2002); [b] The guideline value for uranium is derived from the Guidelines for Drinking-Water Quality (Fourth Edition) (WHO 2011). Abbreviation, bdl refers to below detectable limit. Data exceeding the specified guideline values are indicated in bold italic

(5.63), especially sulfate and Fe concentrations, which were about two orders of magnitude higher than those in natural river water. With increasing distance from the mine and the mixture of other unpolluted streams, the **hydrochemical characteristics** gradually approached normal background levels (e.g., W5). Although, like Stream 1, Stream 2 also passed through the stone coal mining area, it was mainly supplied by the upstream old pit water. Compared to the former, Stream 2 exhibited lower acidity, EC, SO_4^{2-}, and metal concentrations but remained significantly higher than Raobei river water. The maximum U concentration occurred in W6, where the surrounding waste rocks also had a high U concentration (G10, 173 mg kg^{-1}), with a total sulfur content as high as 4.10%, indicating an active acid-producing process (Du et al. 2017).

According to the surface water environmental quality standards in China and the WHO drinking water quality standards, the factors exceeding the limits in the study area's surface water included pH, SO_4^{2-}, F^-, Fe, total P, and U (Table 2). The samples exceeding the standards were mainly pit water and streams passing through the mining area. After flowing into the Raobei River, the river water's (W5) various factors were below the standard limits. The U concentration dropped to 0.128×10^{-2} mg L^{-1}, which was close to the U concentration in the unpolluted upstream river (W8, 0.125×10^{-2} mg L^{-1}).

The mineralogical and geochemical characteristics of sediments

XRD analysis of sediments indicated the absence of carbonate minerals and pyrite (Table 1). However, secondary minerals such as siderite and gypsum were detected. The presence of siderite suggested a high oxidation degree of pyrite (Concas et al. 2006). The appearance of gypsum indicated excess sulfates in Stream 1 (W6), with a sulfate concentration of 5832 mg L^{-1}. The analysis results of pH and partial chemical compositions for five sediment samples are presented in Fig. 2. The pH variation pattern of the sediments was generally consistent with that of the stream and river water. Sediments from the new pit revealed acidity, with a gradual transition to neutrality with increasing distance from the mine. The total sulfur content in the sediments correlated positively with acidity, with the highest value observed in Stream 1 (W6). XRD analysis results indicated that sulfur was primarily present in the form of secondary sulfate minerals, such as gypsum (3.5%). The distribution patterns of Fe and Mn concentrations in the sediments showed differences, with the highest Fe concentration occurring in DW6 and DW7 (both exceeding 14%). Conversely, the Mn concentration at these points was minimal, indicating the predominant precipitation of Fe-bearing minerals in Stream 1 and Stream 2 rather than Mn. The U concentrations decreased progressively from Stream 1 and Stream 2 to the downstream Raobei River. DW6 and DW9, strongly impacted by AMD from new pits, contained U concentrations approximately four times higher than those in sediments from unpolluted samples. The distribution

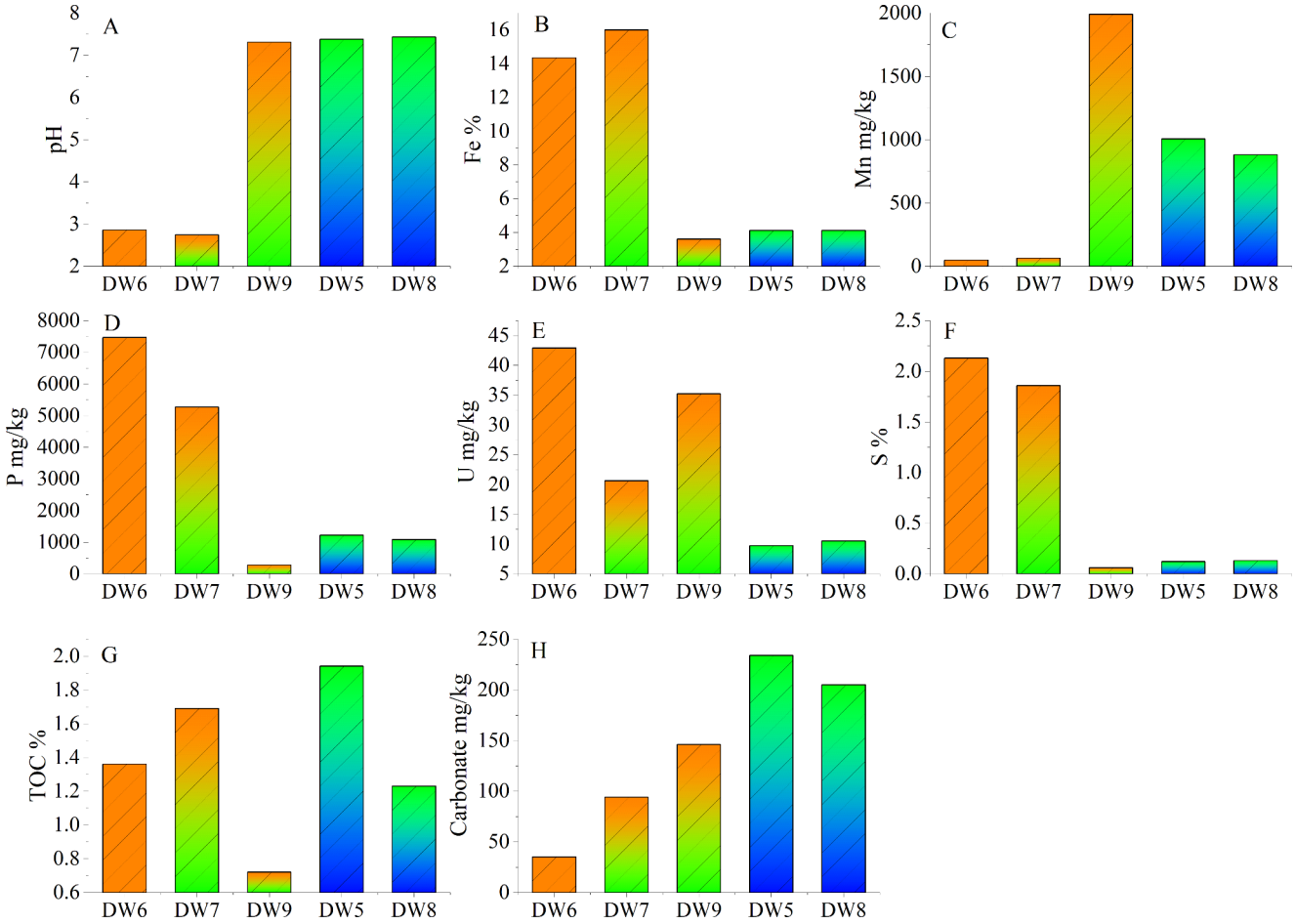

Fig. 2 pH values and the concentrations of major and trace compositions in stream and river sediments

Table 3 Statistical results of pH and uranium concentrations of soil samples ($n=26$)

Parameter	Soil					Background values (Wang et al. 2016)
	Ave	Min	Max	SD	CV	
pH	5.25	2.85	7.02	1.39	0.26	8.0
U (mg kg^{-1})	39.35	2.27	191.0	37.65	0.96	2.5

Abbreviations: Ave, Arithmetic mean; Min, Minimum value. Max, Maximum value. SD, Standard deviation. CV, Coefficient of variation

characteristics of total phosphorus in sediments closely resembled those of U, indicating a positive correlation between the two.

pH and uranium concentrations of soils in the surrounding farmlands of stone coal mine

Table 3 presents the statistical results of soil pH and uranium concentrations in the surrounding farmlands of the mine. Influenced by the acidic drainage from the mine, the soil pH exhibited slight acidity, with a mean value of 5.25, comparable to the reported soil pH (5.59) in the distribution area of black shale in Anji, China (Zhang et al. 2021). Overall, the soil pH in the study area was relatively lower than the national soil background values. The mean, minimum, maximum, standard deviation and coefficient of variation of U concentrations in soil samples are also listed in Table 3. Their spatial distribution is illustrated in Fig. 3. In comparison to the national background value ($n=3382$, 2.5 mg kg^{-1}, referring to Wang et al. 2016), and the regional average in the investigation of natural radiation levels in Shangrao ($n=43$, converted to approximately 3.79 mg kg^{-1} from 55.3 Bq kg^{-1}, referring to Li et al. 1993), the average concentration of U in soil samples exceeded the former two by an order of magnitude. The highest measured value (S2, 191.0 mg kg^{-1}) was about 50 times the background level in the Shangrao region. Similar enrichment of U in soils has been reported in another major stone coal mining area in Xiushui, Jiangxi Province, China (Xu et al. 2018).

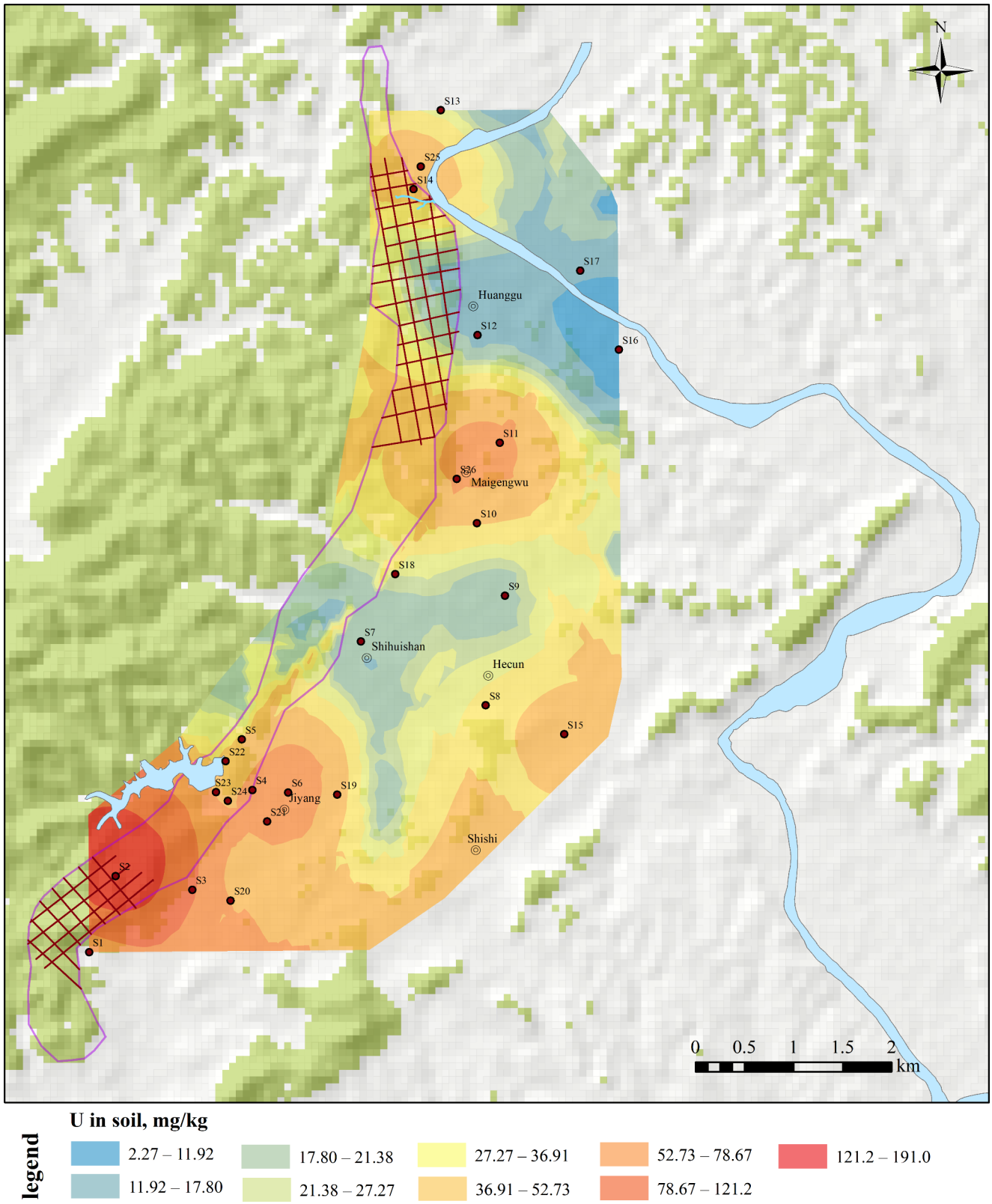

Fig. 3 Distribution of uranium concentrations in farmland soils surrounding the stone coal mine. Other legends are consistent with those in Fig. 1

As depicted in Fig. 3, uranium enrichment was observed in the surrounding farmland soils of the mine. At 57% of the sampling points, uranium concentrations exceeded national background values by tenfold, necessitating considerable attention. The spatial distribution of uranium concentrations revealed that in the proximity of open-pit mining areas, such as Ji Yang, He Cun and Shi Shi, soil uranium concentrations were significantly higher compared to non-mined regions. This implied that stone coal, once exposed to the surface through anthropogenic exploitation, under the influence of AMD, facilitated the release and mobility of uranium (Parviainen and Loukola-Ruskeeniemi 2019; Perkins and Mason 2015). The lower uranium concentrations in weathered waste rocks compared to unweathered waste rocks, as demonstrated in Table S2 of Supplementary material, further supported this inference. The S2, the sample with the highest uranium concentration was situated in an open-pit mining area, representing residual soil formed by the weathering of coal seams as the parent rock. Uranium was similarly enriched in residual soils formed by weathering of the parent rock, influenced by the high uranium concentration in the parent rock (G2, 162 mg kg^{-1}), as reported by Zhang et al. (2021). Therefore, the natural weathering of stone coal represented a significant source of uranium enrichment in farmland soils within the study area. Additionally, the distribution of uranium concentrations in sediments clearly indicated that uranium pollutants from the mining area were spread along the stream through dissolution and transportation (Concas et al. 2006), resulting in widespread soil uranium contamination.

The results of sequential chemical extraction and hydrogeochemical modeling

Utilizing the SCEM, the mode of occurrence of uranium in eight representative samples of waste rocks, soils, and sediments was determined. The specific test results are presented in Fig. 4. Dai et al. (2021) summarized the occurrence of uranium in stone coal, suggesting that uranium was primarily adsorbed to organic matter in the form of uranyl ions, similar to G1, where uranium was predominantly present in an oxidizable fraction (Fig. 4). However, some studies also noted that during the process of sequential chemical extraction, due to the encapsulation of fine minerals by organic matter, uranium present in these stable fine minerals was mistakenly categorized as organically bound, resulting

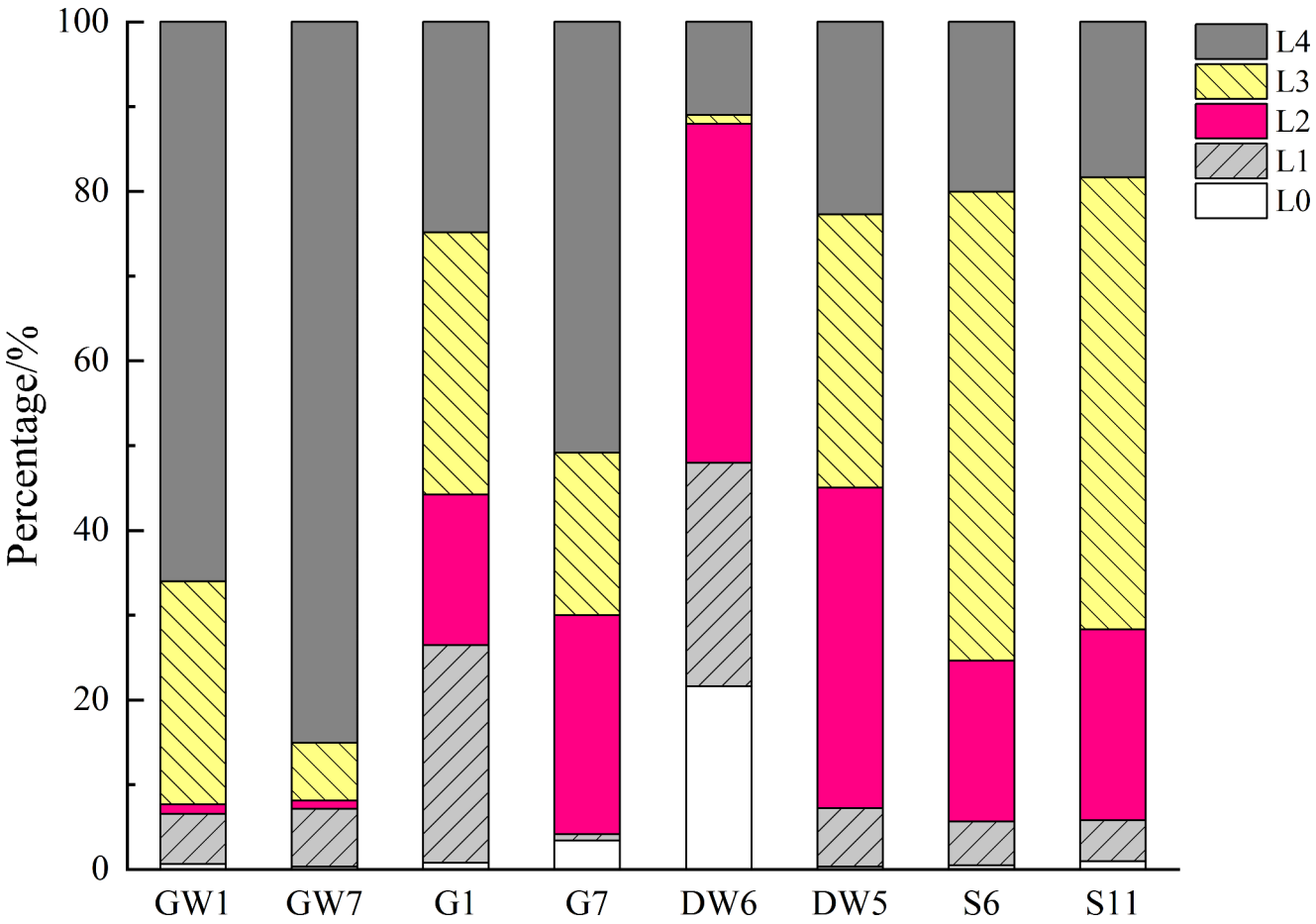

Fig. 4 Sequential chemical extraction results of uranium in waste rock, soil, and sediment samples

in an overestimation of the concentration of organically bound uranium (Dai et al. 2020; Spears 2013). In this study, uranium in waste rocks was also predominantly present in the residual fraction (up to 85.08%), where it was bound within mineral crystalline structures—a highly stable fraction less likely to be released from rocks and unavailable for biological utilization (Zhou et al. 2014; Zhang et al. 2021). Weathered waste rocks (GW1, GW7) exhibited uranium concentrations significantly lower than unweathered waste rocks (Supplementary material, Table S2), but the proportion of the residual fraction was relatively higher, indicating uranium release during weathering (Perkins and Mason 2015). While uranium in waste rocks primarily existed in relatively stable residual or oxidizable fractions, bioavailable fraction ($L_0 + L_1$) also accounted for a certain proportion (4.15–26.44%). Moreover, considering the high total uranium concentrations (Supplementary material, Table S2), the absolute amount of uranium potentially released upon exposure to the surface should not be disregarded.

Sequential chemical extraction results indicated that uranium in the sediments of new pits primarily existed in bioavailable fraction (L_0+L_1, 48%). This fraction of uranium demonstrated strong potential mobility and high environmental risks (Zhou et al. 2014). The significant presence of clay minerals (53.3%) in DW6, in contrast to the geochemical properties of the stone coal waste rocks, implied that these sediments may not have originated from the weathering of the stone coal, but rather have been deposited through external transportation processes. It is worth noting that clay minerals possess a strong capacity for uranium adsorption (Song et al. 2007), and it is plausible that the uranium enrichment observed in the sediments of new pits was primarily attributed to its adsorption onto clay minerals, which can be readily reactivated.

The distribution of uranium in different fractions of soils showed the characteristics of oxidizable fraction > reducible fraction ≈ residual fraction > weak acid-extractable fraction > water-soluble fraction, with the oxidizable state (L_3) accounting for over 50% (Fig. 4). This could be attributed to the enrichment of organic matter in the soils (34.9–103 g kg^{-1}, referring to Yang et al. 2022). A certain proportion of uranium in the soil was also present in the reducible fraction (19.02–22.51%, Fig. 4), indicating that uranium was also associated with iron-manganese (hydro) oxide minerals.

It has been reported that the toxicity of harmful trace elements in water is closely related to their chemical species (Liao et al. 2018). Before the remediation and removal of harmful trace elements from AMD, it is essential to consider their chemical fraction. The PHREEQC hydrogeochemical program is widely used to simulate and calculate the chemical species of ions in water-rock interaction processes, including coal mine waste rocks (Kříbek et al. 2018; Namaghi and Li 2016; Qureshi et al. 2016; Santofimia et al. 2022). In this study, the PHREEQC software was used to determine the chemical species of uranium in AMD, streams, and Raobei river water (Fig. 5b), where uranium predominantly existed as hexavalent (VI) complexes. Figure 5a illustrates a positive correlation between the total amount of uranium and acidity. The AMD, such as W6 with low pH, contained a significantly higher total uranium concentrations. The distribution of uranium species was as follows: UO_2SO_4 > $UO_2(SO_4)_2^{2-}$ > $UO_2(HPO_4)_2^{2-}$ > UO_2^{2+} > UO_2F^+. Santofimia et al. (2022) observed a similar predominance of uranium in the species of UO_2SO_4 (67–71%) in acidic water produced by black shale in the Iberian Massif mountains of Spain. The pH of water samples demonstrated an upward trend upon flowing into the stream, leading to a substantial deposition of U, accompanied by a significant reduction in the total concentrations of U. In nearly neutral streams and river water, the chemical species of uranium experienced a significant change. Uranium was primarily present in the forms of hydrophosphate and carbonate complexes such as $UO_2(HPO_4)_2^{2-}$, $UO_2(CO_3)_2^{2-}$, and UO_2CO_3, which is consistent with the simulated results of neutral drainage from a uranium-containing coal waste pile reported by Kříbek et al. (2018).

The potential environmental risks of uranium

Uranium has been proven to possess developmental toxicity, and inhalation or ingestion of uranium can cause internal irradiation. Additionally, excessive exposure to uranium can also result in chemical toxicity. In some cases, the chemical toxicity of soluble uranium compounds may even exceed their radiotoxicity (Domingo 2001). Due to the elevated U concentrations in stone coal (Dai et al. 2017; Yang et al. 2022), the potential environmental impact of uranium has attracted widespread attention (Wei et al. 2021; Ye et al. 2004; Zhou 1981). Previous studies, although including various media such as coal, ash, soil, water, air, and biota, predominantly focused on the total concentration of uranium, with little consideration for its chemical fractions. Therefore, to more reasonably evaluate the pollution and potential environmental risks of uranium, this study integrated two widely used approaches for quantitatively assessing the potential environmental risk of solid samples, including the I_{geo} and RAC (Dong et al. 2021; Fu et al. 2019; Ma et al. 2020; Wu et al. 2021; Zhang et al. 2022). I_{geo} not only considers the impact of natural geological processes on element background values but also focuses on the influence of human activities on toxic element pollution (Wu et al. 2021). RAC determines the potential environmental risk of toxic metals by determining the proportion of the bioavailable fraction (L_0+L_1). The risk level is determined based

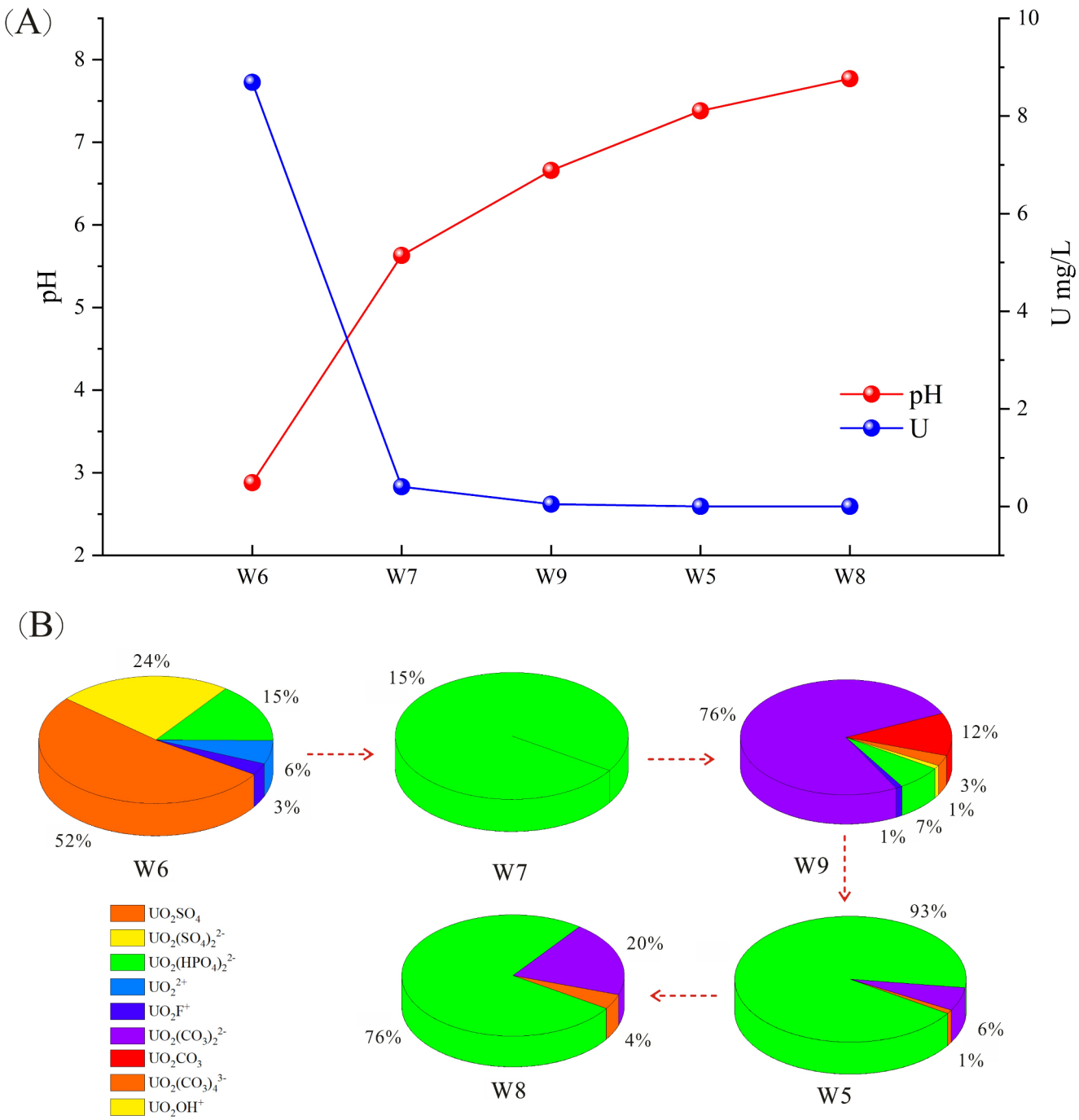

Fig. 5 Correlation between pH and U concentrations (**a**) and the species of uranium in AMD, stream and river water simulated through PHREEQC procedure (**b**)

on the RAC value, classified as < 1%, 1–10%, 11–30%, 31–50%, and > 50%, representing no risk, low risk, moderate risk, high risk, and very high risk, respectively.

The I_{geo} results for uranium of solid samples, including waste rocks, soils, and sediments, are presented in Fig. 6a. The I_{geo} values ranged from −0.72 to 5.74, with average values of 3.88 for waste rocks, 2.99 for soil, and 2.47 for sediment, respectively. According to the I_{geo} values of waste rock samples, 8% of the sampling points were classified as uncontaminated ($I_{geo} = 0$), while other sampling points were mostly heavily or severely polluted. The highest I_{geo} value was S2 (5.67, weathered residual soil of stone coal), and most I_{geo} values of soils ranged from 2 to 4, indicating moderate to strong pollution. The I_{geo} results for sediments showed that heavily polluted samples were primarily concentrated in the streams passing through the mining area.

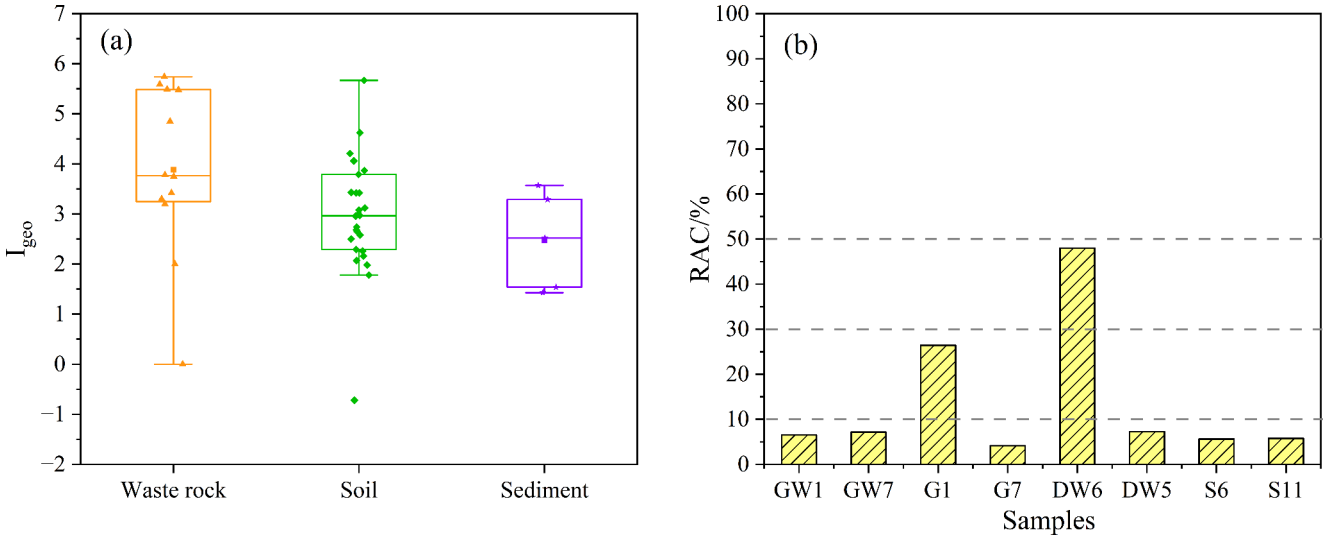

Fig. 6 Results of I_{geo} (**a**) and RAC (**b**) for waste rocks, soils, and sediments in stone coal mining area. $I_{geo} = \log_2(C_n/1.5 \times B_n)$, where C_n is the uranium content in the solid media, and B_n is the background value. Background values for waste rock, soil, and sediment are set at 2.4 mg kg^{-1} (Ketris and Yudovich 2009), 2.5 mg kg^{-1} (Li et al. 1993), and 2.4 mg kg^{-1} (Shi et al. 2016), respectively

These results indicated that abandoned mine represented a significant source of uranium pollution, and long-term weathering had resulted in some degree of contamination in the surrounding environmental media.

The RAC results for the eight solid samples are illustrated in Fig. 6b. The sampling point with the highest RAC value is the sediment from the new pit (DW6, RAC = 48%). In comparison to DW6, the uranium of DW5 was mainly associated with Fe-Mn hydroxides, organic matter, and residual forms, resulting in a low potential risk. The soil in the mining area exhibited a high organic matter content, and most of the uranium was associated with organic matter, resulting in RAC values below 10, indicating a low-risk level for the ecosystem.

The evaluations based on the I_{geo} and RAC indicated a certain degree of U contamination in waste rocks, soils, and sediments. Particularly, in some sampling points, notably in the waste rocks and sediments from the new pits, a considerable amount of bioavailable uranium was observed, suggesting a potential risk of release and mobility.

Discussion

The mode of occurrence of elements and external environmental factors are the two crucial factor for predicting the mobility behavior during the development and utilization of coal resources, as well as the leaching of coal waste during weathering (Finkelman 1995). Leaching tests on stone coal waste rocks from Hubei Province, China, showed that the leaching amount of metal elements (V, Cr, As, Cd, etc.) were not significantly correlated with the total concentrations but were closely related to the concentrations in the water-soluble and exchangeable fractions (Lin et al. 2017). A correlation analysis of U and TOC content was conducted on 55 samples of stone coal-bearing black shales from Enshi, Xiushui, and this research area (Wang et al. 2017; Xue et al. 2018). The results indicated a positive correlation between the concentrations of U and TOC (Fig. 7a). In addition to organic matter, the enrichment of uranium in coal was closely related to the phosphorus (Fig. 7b). Wang et al. (2014) inferred, through electron probe analysis, that the uranium minerals in the black shales of Xiuwu Basin were mainly apatite and phosphorus-containing uranium minerals. Scanning electron microscopy in-situ analysis of Permian uranium-rich black shales in Enshi, Hubei, also found that uranium was associated with phosphorus minerals (such as xenotime and rhabdophane) (Wang et al. 2017). However, in this study, sequential chemical extraction data of waste rocks indicated that U was mainly present in the residual and organic-bound fractions (Fig. 4). It can be inferred that in addition to being associated with organic matter by hexavalent complexes, a portion of uranium in stone coal existed as the tetravalent form in uranium minerals or stable minerals. This is evidenced by the presence of some outliers in Fig. 7a (highlighted with black circles). Based on the spatial distribution characteristics of uranium in environmental media such as water, sediment, and soil, the enrichment of uranium is likely to originate mainly from the weathering and mobility of waste rock. Two pieces of evidences support this: (1) a significant decrease of uranium concentrations in weathered waste rocks samples (Supplementary material, Table S2); (2) the absence of other

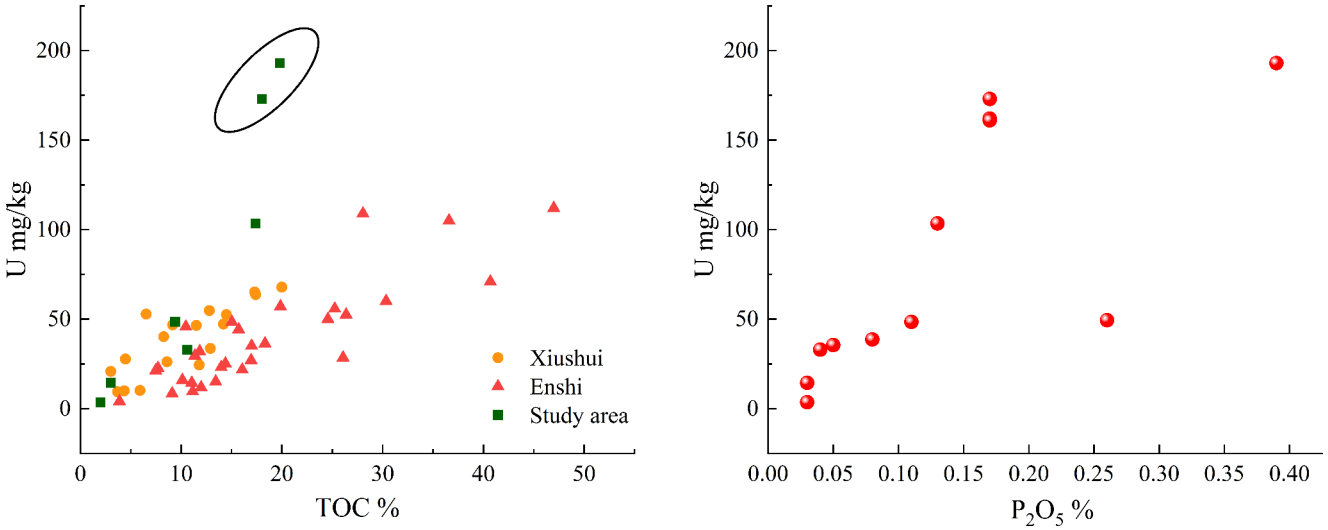

Fig. 7 Scatter plots of uranium concentrations in samples of stone coal-bearing black shales with respect to TOC (**a**) and P_2O_5 (**b**). Data for Enshi and Xiushui are sourced from Wang et al. (2017) and Xue et al. (2018), respectively

industrial activities in the vicinity of the mine that could generate uranium contamination.

The abundant presence of organic matter and sulfide minerals (Supplementary material, Tables S2) make coal and waste rock susceptible to chemical weathering effects (Parviainen and Loukola-Ruskeeniemi 2019). When coal is exposed to the surface, sulfide minerals are prone to oxidation and dissolution, generating AMD with high concentrations of Fe, sulfate, and low pH, accompanied by the release and mobilization of uranium (Saria et al. 2006). A comparison of the sequential chemical extraction results for unweathered and weathered waste rocks revealed that the significant reductions in the uranium concentrations were oxidizable, reducible, and weak acid-extractable fractions. The release of uranium primarily occurred under oxidative and strongly acidic conditions, transforming uranium associated with organic matter and Fe-Mn (hydro) oxide minerals into soluble uranyl sulfate complexes. Similar uranium leaching behavior was observed by Yu et al. (2014) through laboratory oxidation experiments and SCEM. As AMD flowed into Stream 2, the pH of the water increased to 5.63, leading to significant precipitation and enrichment of uranium in the sediments (Fig. 5a). Simultaneously, there was a notable change in the species of uranium, shifting from sulfate complexes to hydrophosphate and carbonate complexes. Kříbek et al. (2018) summarized four ways in which polluted water transfers pollutants to sediments, including adsorption on mineral surfaces, organic matter adsorption complexes, coprecipitation with iron-manganese hydroxides, phosphates, carbonates, and forming independent minerals. As shown in Fig. 2, the uranium concentrations in the sediments were positively correlated with total phosphorus and iron, indicating coprecipitation of uranium with phosphate and iron hydroxides.

Fig. 8 summarizes the mobility patterns of uranium from stone coal mine under surface weathering. Firstly, uranium-rich waste rocks containing high organic matter and pyrite were exposed to the surface through human mining activities, leading to the oxidation and dissolution of pyrite, and then generating AMD. As the composition of stone coal is heterogeneous, varying in different regions or even within the same mining area, the sulfide minerals, associated metal elements, and host rocks differ significantly (Parviainen and Loukola-Ruskeeniemi 2019). In this respect, the content of carbonate minerals in the host rocks can affect their acid-producing capacity. Lin et al. (2017) found through laboratory leaching experiments with stone coal waste rocks that waste rocks possessed acid neutralization capacity, with the pH stabilizing between 8.3 and 8.5 under different initial pH conditions (ranging from 3 to 9). In this study, consistent acid neutralization phenomena was observed in some coal waste rocks, such as in some water samples collected from the old pits (W2, W3, and W4), which showed near-neutral acidity, with pH values of 7.38, 6.93, and 7.05, respectively (Table 2), indicating that weak capacity of acid production and low environmental risk.

Secondly, uranium in stone coal was partly associated with organic matter in hexavalent form, and the other part was present in tetravalent form in stable minerals (such as phosphorus-containing minerals). Under strong acidic and oxidative conditions, uranium was leached by AMD, forming soluble species like UO_2SO_4, $UO_2(SO_4)_2^{2-}$, and minor amounts of $UO_2(HPO_4)_2^{2-}$, UO_2^{2+}, and UO_2F^{+}. After AMD flowing into stream, it was diluted, resulting in a gradual increase in pH and then the concentrations of sulfate, iron,

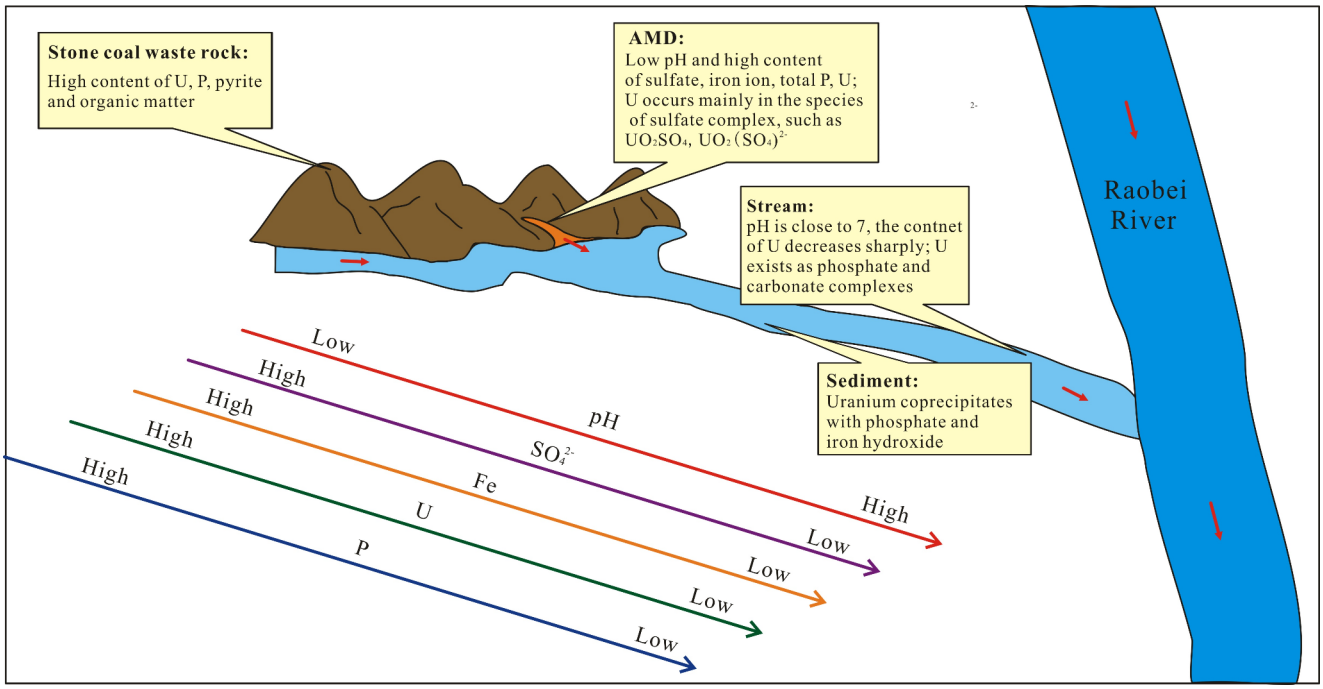

Fig. 8 The mobility pattern of uranium within the stone coal mining region

phosphorus, and uranium decreased progressively. Simultaneously, corresponding sediments showed a gradual decline in the concentrations of these elements, with uranium primarily co-precipitating with phosphate and iron hydroxides. Finally, the uranium concentrations in downstream river waters sharply decreased to near background levels, below environmental standard limits. The species of uranium shifted predominantly to hydrophosphate and carbonate complexes. It reflected the process of natural attenuation of pollutants (He et al. 2019).

In accordance with the mobility pattern of uranium under weathering in abandoned stone coal mines, the following measures and strategies are proposed to mitigate the risks: (1) Implementing physical barriers such as clay, geofabric film, gravel, and soil to impede oxygen and surface water infiltration, thereby slowing down waste rock oxidation and acid generation, and regulating the release of uranium from their source; (2) Raising the pH of water in AMD-affected effluents through the addition of alkaline chemicals (Acharyaa and Kharelb 2020), such as calcium hydroxide ($Ca(OH)_2$), calcium oxide (CaO), sodium hydroxide (NaOH), sodium carbonate (Na_2CO_3), and ammonia (NH_3), resulting in the formation of precipitates from dissolved iron and phosphate, which can adsorb and subsequently remove uranium by co-precipitation. A recent study also suggested that dumping building debris at AMD sites not only neutralizes the acidity of AMD, but also frees up landfill space by removing concrete waste (Rezaie and Anderson 2020). The implementation of an ecological restoration engineering at an abandoned stone coal mine in Yiyang, Hunan province, China, has also demonstrated effectiveness in controlling pollution (Peng et al. 2021). Duo to the heterogeneity of waste rock, each mining project is unique. Consequently, the formulation of risk mitigation strategies may vary depending on factors such as the location, land use history, available technology, ecohydrological environment, socio-economic conditions, and political outlook (Acharyaa and Kharelb 2020). Further research is required to develop risk mitigation measures for the currently studied abandoned mines. In any case, however, ongoing environmental monitoring of mines sites is necessary.

Conclusion

This study investigated the occurrence, mobility behavior, and potential environmental risk of uranium in waste rocks, soil, sediments, and surface water in an abandoned stone coal mining area of Jiangxi Province, China. The results indicated that the abandoned open-pit mine represented the primary source of uranium pollution. The self-purification and natural attenuation of streams were observed. Both sediments and surface water showed similar geochemical characteristics, with high uranium concentrations only occurring near the mine. In contrast, uranium-rich soils were more widely distributed in the downstream watershed of mine.

The mode of occurrence and external environment conditions determined the mobility of uranium.

Uranium in waste rocks was leached by AMD to form soluble uranium sulfate complexes. As AMD flowed into nearly neutral streams, a significant amount of uranium precipitated with phosphates and iron hydroxides, leading to a transformation in the uranium species, with hydrophosphate and carbonate complexes becoming predominant. There is a substantial amount of uranium present in the bioavailable fraction (L_0+L_1) in unweathered waste rocks and sediments from the new pits, having a relatively high potential environmental risk. Further research should focus on laboratory leaching tests to assess the release rate of uranium. Such tests can provide specific information to understand the release and mobility behavior of uranium under different conditions (Petrovic and Fiket 2022). Due to the heterogeneity of the waste rock, it is important to understand the mode of occurrence of uranium, acid-producing capacity, and environmental conditions before developing a mine remediation strategy.

Supplementary Information The online version contains supplementary material available at https://doi.org/10.1007/s12665-024-11799-5.

Acknowledgements This research was financially supported by "Mechanism of in situ bio-desulfurization and uranium immobilization of acidic uranium-bearing groundwater" (No. 2022NRE-LH-20), jointly foundation funded by China National Uranium Corporation Limited & State Key Laboratory of Nuclear Resources and Environment of East China University of Technology.

Author contributions Xinxiang Wei: Writing-original draft preparation. Naizheng Xu: Writing-Reviewing and Editing. Jiang Li: Supervision, Validation. Jianguang Chen: Funding acquisition. Li Chen: Software, Investigation.

Funding This research was financially supported by "Mechanism of in situ bio-desulfurization and uranium immobilization of acidic uranium-bearing groundwater" (No. 2022NRE-LH-20), jointly foundation funded by China National Uranium Corporation Limited & State Key Laboratory of Nuclear Resources and Environment of East China University of Technology.

Data availability No datasets were generated or analysed during the current study.

Declarations

Ethics approval and consent to participate This is an observational study. No ethical approval is required.

Consent to publish The participant has consented to the submission of the case report to the journal

Competing interests The authors declare no competing interests.

References

Acharyaa B, Kharelb G (2020) Acid mine drainage from coal mining in the United States–An overview. J Hydrol 588:1–14. https://doi.org/10.1016/j.jhydrol.2020.125061

Awan R, Liu C, Gong H, Dun C, Tong C, Chamssidini L (2020) Paleosedimentary environment in relation to enrichment of organic matter of Early Cambrian black rocks of Niutitang formation from Xiangxi area China. Mar Petrol Geol 112:104057. https://doi.org/10.1016/j.marpetgeo.2019.104057

Chen J, Chen P, Yao D, Huang W, Tang S, Wang K, Liu W, Hua Y, Lia Q, Wang R (2017) Geochemistry of uranium in Chinese coals and the emission inventory of coal-fired power plants in China. Int Geol Rev 60(5–6):621–637. https://doi.org/10.1080/00206814.2017.1295284

Chou CL (2012) Sulfur in coals: a review of geochemistry and origins. Int J Coal Geol 100:1–13. https://doi.org/10.1016/j.coal.2012.05.009

Concas A, Ardau C, Cristini A, Zuddas P, Cao G (2006) Mobility of heavy metals from tailings to stream waters in a mining activity contaminated site. Chemosphere 63(2):244–253. https://doi.org/10.1016/j.chemosphere.2005.08.024

Dai S, Zheng X, Wang X, Finkelman RB, Jiang Y, Ren D, Yan X, Zhou Y (2017) Stone coal in China: a review. Int Geol Rev 60(5–6):736–753. https://doi.org/10.1080/00206814.2017.1378131

Dai S, Hower J, Finkelman R, Graham I, French D, Ward C, Eskenazy G, Wei Q, Zhao L (2020) Organic associations of non-mineral elements in coal: a review. Int J Coal Geol 218:103347. https://doi.org/10.1016/j.coal.2019.103347

Dai S, Finkelman R, French D, Hower J, Graham I, Zhao F (2021) Modes of occurrence of elements in coal: a critical evaluation. Earth Sci Rev 222:103815. https://doi.org/10.1016/j.earscirev.2021

Domingo J (2001) Reproductive and developmental toxicity of natural and depleted uranium: a review. Reprod Toxicol 15(6):603–609. https://doi.org/10.1016/S0890-6238(01)00181-2

Dong YB, Liu Y, Lin H (2018) Leaching behavior of V, pb, cd, cr, and as from stone coal waste rock with different particle sizes. Int J Min Met Materi 25(8):861–870. https://doi.org/10.1007/s12613-018-1635-2

Dong L, He Z, Zhang F, Xu T, Wu J, Yan K, Pan X, Zhang D (2021) Assessment of uranium migration and pollution sources in river sediments of the Ili River Basin using multiply statistical techniques. Environ Sci Pollut Res Int 28(5):5372–5382. https://doi.org/10.1007/s11356-020-10887-w

Du Z, Hao C, Pei C, Wei P, Zhang Y, Lv Y (2017) Molecular research of acid-generating microbial communities in abandoned ores in the waste dump of an iron mine in Anhui Province. Environ Sci 38(11):4725–4732. https://doi.org/10.13227/j.hjkx.201704047

Finkelman R (1995) Modes of occurrence of environmentally-sensitive trace elements in coal. Springer, Dordrecht

Fu B, Liu G, Mian MM, Sun M, Wu D (2019) Characteristics and speciation of heavy metals in fly ash and FGD gypsum from Chinese coal-fired power plants. Fuel 251:593–602. https://doi.org/10.1016/j.fuel.2019.04.055

Guo Z (1990) Problems of stone coal resources and comprehensive development in Jiangxi Province. Jiangxi Energy (3): 4–8

He J, Li W, Liu J, Chen S, Frost R (2019) Investigation of mineralogical and bacteria diversity in Nanxi River affected by acid mine drainage from the closed coal mine: implications for characterizing natural attenuation process. Spectrochim Acta A 217:263–270. https://doi.org/10.1016/j.saa.2019.03.069

Huang Y, Li J, Song T, Sun Q, Kong G, Wang F (2017) Microstructure of coal gangue and precipitation of heavy metal elements. J Spectrosc 2017:1–9. https://doi.org/10.1155/2017/3128549

Indigofera amblyantha craib for ecological restoration of rock slopes in stone coal mine. Adsorpt Sci Technol (2021) https://doi.org/10.1155/2021/3827991
Ketris M, Yudovich Y (2009) Estimations of clarkes for carbonaceous biolithes: World averages for trace element contents in black shales and coals. Int J Coal Geol 78(2):135–148. https://doi.org/10.1016/j.coal.2009.01.002
Kříbek B, Sracek O, Mihaljevič M, Knésl I, Majer V (2018) Geochemistry and environmental impact of neutral drainage from an uraniferous coal waste heap. J Geochem Explor 191:1–21. https://doi.org/10.1016/j.gexplo.2018.05.001
Lavergren U, Åström ME, Bergbäck B, Holmström H (2009) Mobility of trace elements in black shale assessed by leaching tests and sequential chemical extraction. Geochem Explor Environ Anal 9(1):71–79. https://doi.org/10.1144/1467-7873/08-188
Li X, Zheng S, Wu X, Li Y, Sun S, Yang M, Wan M, Zhang S (1993) Investigation of natural radionuclide contents in soil in Jiangxi Province. Radiat Prot (4):291–294
Liao F, Wang G, Shi Z, Huang X, Xu F, Xu Q, Guo L (2018) Distributions, sources, and species of heavy metals/trace elements in shallow groundwater around the Poyang Lake, East China. Expos Health 10:211–227. https://doi.org/10.1007/s12403-017-0256-8
Lin H, Li G, Dong Y, Li J (2017) Effect of pH on the release of heavy metals from stone coal waste rocks. Int J Min Process 165:1–7. https://doi.org/10.1016/j.minpro.2017.05.001
Ma W, Liu S, Li Z, Li Zhen, Lv J, Yang L (2020) Release and transformation mechanisms of hazardous trace elements in the ash and slag during underground coal gasification. Fuel 281:118774. https://doi.org/10.1016/j.fuel.2020.118774
Namaghi H, Li S (2016) Acid-generating and leaching potential of soils in a coal waste rock pile in Northeastern China. Soil Sediment Contam 25(7):776–791. https://doi.org/10.1080/15320383.2016.1213701
Parviainen A, Loukola-Ruskeeniemi K (2019) Environmental impact of mineralised black shales. Earth Sci Rev 192:65–90. https://doi.org/10.1016/j.earscirev.2019.01.017
Peng B, Song Z, Tu X, Xiao M, Wu F, Lv H (2004) Release of heavy metals during weathering of the Lower Cambrian black shales in western Hunan, China. Environ Geol 45(8):1137–1147. https://doi.org/10.1007/s00254-004-0974-7
Peng L, Mao Q, Cao L, Sun H, Xie X, Luo S (2021) Insight into the adaptability of dominant plant
Perkins R, Mason C (2015) The relative mobility of trace elements from short term weathering of a black shale. Appl Geochem 56:67–79. https://doi.org/10.1016/j.apgeochem.2015.01.014
Petrovic M, Fiket Z (2022) Environmental damage caused by coal combustion residue disposal: a critical review of risk assessment methodologies. Chemosphere 299:134410. https://doi.org/10.1016/j.chemosphere.2022.134410
Qi F, Zhang Z, Li Z, Wang Z, He Z, Wang W (2011) Unconventional uranium resources in China. Uranium Geol 27(04):193–199
Qureshi A, Maurice C, Öhlander B (2016) Potential of coal mine waste rock for generating acid mine drainage. J Geochem Explor 160:44–54. https://doi.org/10.1016/j.gexplo.2015.10.014
Rauret G, Rubio R, López-Sánchez J (1989) Optimization of Tessier procedure for metal solid speciation in river sediments. Int J Environ Ch 36(2):69–83. https://doi.org/10.1080/03067318908026859
Rezaie B, Anderson A (2020) Sustainable resolutions for environmental threat of the acid mine drainage. Sci Total Environ 717:137211. https://doi.org/10.1016/j.scitotenv.2020.137211
Santofimia E, González F, Rincón-Tomás B, López-Pamo E, Marino E, Reyes J, Bellido E (2022) The mobility of thorium, uranium and rare earth elements from Mid Ordovician black shales to acid waters and its removal by goethite and schwertmannite. Chemosphere 307:135907. https://doi.org/10.1016/j.chemosphere.2022.135907
Saria L, Shimaoka T, Miyawaki K (2006) Leaching of heavy metals in acid mine drainage. Waste Manage Res 24(2):134–140. https://doi.org/10.1177/0734242X06063052
Shi C, Liang M, Feng B (2016) Average background values of 39 chemical elements in stream sediments of China. Earth Sci 41(02):234–251. https://doi.org/10.3799/dqkx.2016.018
Song D, Qin Y, Zhang J, Wang W, Zheng C (2007) Concentration and distribution of trace elements in some coals from northern China. Int J Coal Geol 69(3):179–191. https://doi.org/10.1016/j.coal.2006.08.005
Spears DA (2013) The determination of trace element distributions in coals using sequential chemical leaching—A new approach To an old method. Fuel 114:31–37. https://doi.org/10.1016/j.fuel.2012.09.028
Steiner M, Wallis E, Erdtmann B, Zhao Y, Yang R (2001) Submarine-hydrothermal exhalative ore layers in black shales from South China and associated fossils; insights into a Lower Cambrian facies and bio-evolution. Palaeogeogr Palaeocl 169(3–4):165–191. https://doi.org/10.1016/S0031-0182(01)00208-5
Sun Y, Xiao K, Wang X, Lv Z, Mao M (2020) Evaluating the distribution and potential ecological risks of heavy metal in coal gangue. Environ Sci Pollut R 28(15):18604–18615. https://doi.org/10.1007/s11356-020-11055-w
Wang Y, Hu B, Gao H, Li W, Bai H, Guo G (2014) The lithogeochemical characteristics and tectonic environment of archie mountain granite pluton. Xinjiang Uranium Geol 30(01):1–6. https://doi.org/10.3969/j.issn.1000-0658.2014.01.001
Wang X, Zhou J, Xu S, Chi Q, Nie L, Zhang B, Yao W, Wang W, Liu H, Liu D, Han Z, Liu Q (2016) China soil geochemical baselines networks: data characteristics. Geol China 43(05):1469–1480. https://doi.org/10.12029/gc20160501
Wang X, Tang Y, Jiang Y, Xie P, Zhang S, Chen Z (2017) Mineralogy and geochemistry of an organic- and V-Cr-Mo-U-rich siliceous rock of late Permian age, western Hubei Province, China. Int J Coal Geol 172:19–30. https://doi.org/10.1016/j.coal.2016.12.006
Wang X, Li P, Liu Y, Sun Z, Chai L, Min X, Guo Y, Zheng Z, Ke Y, Liang Y (2018) Uranium bioleaching from low-grade carbonaceous-siliceous-argillaceous type uranium ore using an indigenous *Acidithiobacillus ferrooxidans*. J Radioanal Nucl Chem 317(2):1033–1040. https://doi.org/10.1007/s10967-018-5957-3
Wei X, Li J (2023a) Research progress on environmental impact of uranium migration during development and utilization of coal resources. Sci Technol Eng 23(10):4033–4043
Wei X, Li J (2023b) Environmental impact and control factors on uranium leaching and release from stone coal under water-rock interaction. Nonferr Met 1163–75. https://doi.org/10.3969/j.issn.1007-7545.2023.11.009
Wei X, Zhang L, Kuang F, Xu N (2021) Investigation of natural radioactive environment in a bone coal mine area, in She County, Anhui Province. Radiat Prot 41(04):343–350
WHO (2011) Guideline for drinking water quality. WHO Press,Geneva
Wu D, Wang Y, Wang M, Wei C, Hu G, He X, Fu W (2021) Basic characteristics of coal gangue in a small-scale mining site and risk assessment of radioactive elements for the surrounding soils. Minerals 11(6):647. https://doi.org/10.3390/min11060647
Xu N, Wei X, Kuang F, Zhang L, Liu H (2018) Study on the natural radioactivity level of stone coal-bearing strata in east China. Environ Earth Sci 77(21):1–11. https://doi.org/10.1007/s12665-018-7916-2
Xue W, Ling H, Li D, Wei W, Wei G, Gao M (2018) Study on characteristics of Lower Cambrian strata and genesis of uranium enrichment/mineralization in the strata in Xiushui area. Geol J China Univ 24(02):210–221. https://doi.org/10.16108/j.issn1006-7493.2017065
Yang Z, Zhang W, Wu W, Ma Z, Li H, Zhang L (2022) Study on remediation of radioactive-heavy metal contaminated soil in stone

coal mines by chemical elution. Coal Sci Technol 50(9):261–266. https://doi.org/10.13199/j.cnki.cst.2021-0041

Ye J, Kong L, Li Y, Zhang L, Jiang S (2004) Study of radioactivity effect of mining and utilizing bone-coal mine on environment. Radiat Prot 24(01):1–23

Yu C, Lavergren U, Peltola P, Drake H, Bergback B, Astrom M (2014) Retention and transport of arsenic, uranium and nickel in a black shale setting revealed by a long term humidity cell test and sequential chemical extractions. Chem Geol 363:134–144. https://doi.org/10.1016/j.chemgeo.2013.11.003

Zhang Q (2000) Uraniferous black shale and related uranium mineralization features in South China. Acta Geol Sin 74(3):602–604

Zhang S, Xu Y, Wu M, Mao X, Yao Y, Shen Q, Zhang M (2021) Geogenic enrichment of potentially toxic metals in agricultural soils derived from black shale in northwest Zhejiang, China: pathways to and risks from associated crops. Ecotoxicol Environ Saf 215:112102. https://doi.org/10.1016/j.ecoenv.2021.112102

Zhang Z, Wang Y, Zhang Y, Shen B, Ma J, Liu L (2022) Stabilization of heavy metals in municipal solid waste incineration fly ash via hydrothermal treatment with coal fly ash. Waste Manage 144:285–293. https://doi.org/10.1016/j.fuel.2019.04.055

Zhao H, Feng C, Liu S, Liu F (2023) Organic geochemical characteristics of Lower Cambrian black rock series in Ziyang, Shanxi Province. J Jilin Univ (Earth Sci Edition) 53(4):1016–1032. https://doi.org/10.13278/j.cnki.jjuese.20220105

Zhou Z (1981) Radiological protection in mining and utilization of uraniferous stone coal is discussed. Radiat Prot 05:74–78

Zhou C, Liu G, Wu D, Ting F, Wang R, Fan X (2014) Mobility behavior and environmental implications of trace elements associated with coal gangue: a case study at the Huainan Coalfield in China. Chemosphere 95:193–199. https://doi.org/10.1016/j.chemosphere.2013.08.065